Carbohydrate Research 451 (2017) 42–50

Contents lists available at ScienceDirect

Carbohydrate Research

journal homepage: www.elsevier.com/locate/carres

Limitations in the description of conformational preferences of *C*-disaccharides: The (1 → 3)-*C*-mannobiose case

Ivan Raich [a], Zuzana Lövyová [a], Ladislav Trnka [a], Kamil Parkan [a, b], Jiří Kessler [b], Radek Pohl [b], Jakub Kaminský [b, *]

[a] University of Chemistry and Technology Prague, Technická 5, 166 28 Prague, Czech Republic
[b] Institute of Organic Chemistry and Biochemistry AS CR, Gilead Sciences & IOCB Research Center, Flemingovo nám. 2, 166 10 Prague, Czech Republic

ARTICLE INFO

Article history:
Received 16 July 2017
Received in revised form
7 September 2017
Accepted 11 September 2017
Available online 18 September 2017

Keywords:
C-disaccharides
Mannosides
Conformations
NMR
J-coupling constants
Molecular dynamics

ABSTRACT

Conformational preferences of two *C*-glycosyl analogues of Man*p*-(1 → 3)-Man*p*, were studied using a combined method of theoretical and experimental chemistry. Molecular dynamics was utilized to provide conformational behavior along *C*-glycosidic bonds of methyl 3-deoxy-3-*C*-[(α-D-mannopyranosyl) methyl]-α-D- and L-mannopyranosides. The OPLS2005 and Glycam06 force fields were used. Simulations were performed with explicit water (TIP3P) and methanol. Results were compared with a complete conformational scan at the MM4 level with the dielectric constant corresponding to methanol. In order to verify predicted conformational preferences, vicinal $^{3}J_{HH}$ NMR coupling constants were calculated by the Karplus equation on simulated potential energy surfaces (PES). A set of new parameters for the Karplus equation was also designed. Predicted $^{3}J_{HH}$ were compared with experimental data. We also used reverse methodology, in which the $^{3}J_{HH}$ coupling constants were calculated at the DFT level for each family of (ϕ, ψ)-conformers separately and then experimental values were decomposed onto calculated $^{3}J_{HH}$ couplings in order to obtain experimentally derived populations of conformers. As an alternative method of evaluation of preferred conformers, analysis of sensitive ^{13}C chemical shifts was introduced. We were able to thoroughly discuss several fundamental issues in predictions of preferred conformers of *C*-saccharides, such as the solvent effect, reliability of the force field, character of empirical Karplus equation or applicability of NMR parameters in predictions of conformational preferences in general.

1. Introduction

Carbohydrates are natural compounds having many important functions in living organisms. They participate in numerous biological processes, where specific recognition of sugar molecules is required. This involves binding to carbohydrate-binding proteins, lectins that control various biological functions including the cell-cell interaction, inflammatory and immune response, fertilization, adhesion and virulence of pathogens [1–3]. DC-SIGN was found important as it serves e.g. as a mediator of transmigration from blood to lymphoid tissue, immunological synapse initiator etc. [4–9] Several pathogens (HIV, Ebola, Dengue, HPVC, *Helicobacter pylori*, *Klebsiella pneumonia* and *Mycobacterium tuberculosis*, *Lishmania pifanoi* or *Schistosoma mansoni*, and *Candida albicans*), however, exploit DC-SIGN to avoid the immune response and invade the host [10–13]. Therefore, inhibiting the interaction of DC-SIGN with a pathogen sugar epitope might be a promising strategy of prophylaxis for which efficient DC-SIGN antagonists need to be developed [11,14].

It has been reported that DC-SIGN specifically binds D-mannose-containing glycans [15–17]. It has been reported that the presence of multiple binding modes increases affinity of the ligand. For example, α-D-Man*p*-(1 → 2)-α-D-Man*p* is bound to DC-SIGN more strongly than simple D-mannose [18]. Several mannose-based glycomimetics have been prepared and their binding affinities studied up to now [19–24]. Nevertheless, a majority of DC-SIGN ligands retain metabolically unstable glycosidic bonds. By contrast, *C*-glycosides, disaccharides or oligosaccharides in which the interglycosidic oxygen atom connecting two monosaccharide units is replaced with a methylene group, exhibit stability against chemical and enzymatic hydrolysis [25].

Lack of *exo*- and *endo*-anomeric effects open questions about their conformational preferences that might influence their affinity

* Corresponding author.
E-mail address: kaminsky@uochb.cas.cz (J. Kaminský).

https://doi.org/10.1016/j.carres.2017.09.006
0008-6215/

to lectins [26–31]. In a pioneering work of Kishi it was postulated that preferred conformations of *C*-disaccharides are similar to their *O*-counterparts [32–35]. However, it was later shown that this assumption based on semi quantitative analysis of NMR data should be complemented by molecular modeling calculations [36] in order to cover all possible conformers present in solution. The complete conformational analysis identifying all possible conformations seems to be important because in some cases a less populated (unbound state) conformer can be preferentially recognized by a protein as was discovered for *C*-glycosyl derivative of β-1,3-linked lactose derivative bound by human lectin galectin-1 [37].

The analysis of several NMR parameters (indirect spin-spin coupling constants, NOE, residual dipolar couplings, ^{13}C chemical shifts) coupled with molecular modeling still represent the state-of-the-art method for conformational studies. Recent advances in solvated theoretical simulations combined with high-field and isotopically-enriched NMR spectroscopy have proven their ability to provide a detailed information about the conformational behavior of saccharides. Nevertheless, the conformation of *C*-disaccharides has been explored only for few representatives of disaccharide links and monosaccharide configurations (α-D-Man*p*-(1 → 1)-β-D-Gal*p* [38], β-D-Gal*p*-(1 → 1)-α-D-Man*p* [39], α-D-Man*p*-(1 → 2)-α-D-Man*p*(1→ [40], β-D-Gal*p*-(1 → 3)-β-D-Glc*p*(1→ [41], and β-D-Gal*p*-(1 → 4)-β-D-Glc*p*(1→. [36,42]).

The α-D-Man*p*-(1 → 3)-α-D-Man*p* motifs can be found as a part of cell surface carbohydrates as the core branching region of asparagine-linked oligosaccharides. Conformational behavior of α-D-Man*p*-(1 → 3)-α-D-Man*p*, as well as its (1 → 6) analog in water was partly studied by Mikkelsen et al. [43] In the present paper we report a conformational study of *C*-analog of α-D-Man*p*-(1 → 3)-α-D-Man*p*OMe (methyl 3-deoxy-3-*C*-[(α-D-mannopyranosyl)methyl]-α-D-mannopyranoside, **1**, see Fig. 1) and *C*-analog of α-D-Man*p*-(1 → 3)-α-L-Man*p*OMe (methyl 3-deoxy-3-*C*-[(α-D-mannopyranosyl)methyl]-α-L-mannopyranoside, **2**) combining methods of molecular mechanics (MM), molecular dynamics (MD) and density functional theory (DFT) coupled with analysis of NMR indirect $^{3}J_{HH}$ spin-spin coupling constants.

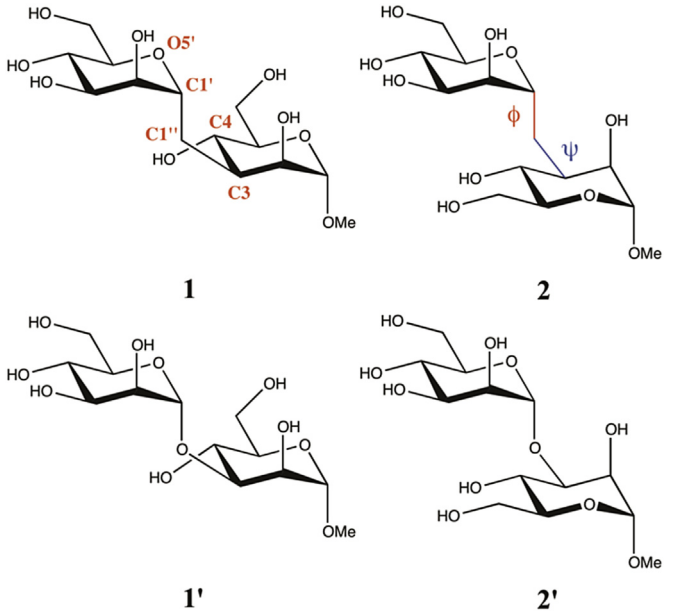

Fig. 1. Studied compounds **1** and **2** (top row), as well as their *O*-analog **1′** and **2′**, and the ϕ, ψ torsion angles definition with atom numbering.

2. Methods

2.1. Materials

Compounds **1** and **2** were prepared as described before from mannopyranosyl ethanal by stereoselective cycloaddition reactions with *R*- and *S*-methyl (ethenyloxy)(phenyl)acetates followed by epoxidation of diastereoisomeric 3-*C*-mannosylated 1,2-glucals [44]. The natural *O*-analog **1′** was purchased from Carbosynth. Similar analog **2′** could not be obtained.

2.2. NMR experiment

^{1}H and ^{13}C (300 and 500 MHz) NMR spectra of **1** and **2** in CD_3OD were recorded on Varian Oxford 300 and Bruker Avance III HD spectrometers and referenced to solvent signal ($\delta(H) = 3.31$ ppm, $\delta(C) = 49.0$ ppm). The assignments of signals were confirmed by homonuclear COSY and heteronuclear 2D correlated spectra.

2.3. Systematic mapping

The systematic mapping of conformational spaces of compounds **1** and **2** was performed at the molecular mechanics level with MM4 force field [45,46]. Three starting orientations (−sc, +sc, ap) were considered for the hydroxymethyl group and the anomeric methoxy group, and two orientations (clockwise or anticlockwise) for each secondary hydroxy group on both monosaccharide subunits. The notation + *sc* refers to the positive synclinal (+*gauche*, ~60°) orientation, −*sc* is the negative synclinal (-*gauche*, ca. −60°) orientation and *ap* stands for the antiperiplanar (*trans*, ~180°) orientation. All combinations of the starting orientations were taken into account and adiabatic maps for torsions ϕ and ψ were constructed with 20° steps giving 34992 starting geometries for each structure. In all calculations, the dielectric constant (ε) was set to 32.6 mimicking thus the methanol environment. The convergence criterion was based on energy differences between two subsequent optimization steps (ΔE threshold of 8×10^{-5} N kcal/mol), where N is the number of atoms in the molecule.

2.4. Molecular dynamic simulation (MD)

Two molecular mechanic force fields (GLYCAM06 [47] and OPLS_2005 (updated parameter set of Jorgensen's OPLS_AA [48])) were used to investigate structural deviations of compounds **1** and **2** caused by the temperature motion and explicit interaction with solvent by MD simulations. One molecule of sugar derivative was placed into the cubic periodic box of water (24.1 Å a side) and surrounded by ~440 TIP3P water molecules. A molecule in methanol box of the equivalent size (22.9 Å a side, ~170 MeOH molecules) was also simulated. A short heating of the system from 0 to 300 K for 20 ps under NVT conditions and 100 ps NpT equilibration preceded the production run, performed for 300 ns under the NpT conditions at the temperature of 300 K, pressure of 1 atm, and 1 fs integration step. A snapshot geometry was sampled each 2 ps. Potential energy surface maps along the ϕ, ψ torsion angles were obtained from incidence probabilities of individual values:

$$E = -RT \ln p, \quad (1)$$

where R is the gas constant, T absolute temperature and p probability of incidence of individual torsion angle value.